Electronic Supplementary Material (ESI) for Physical Chemistry Chemical Physics.

Electronic Supplementary Information

The L-G Phase Transition in Binary Cu-Zr Metallic Liquids

Qi An[a*], William L. Johnson[b*], Konrad Samwer[b,c], Sydney L. Corona[b], Yidi Shen[a], and William A. Goddard III[d*]

[a]Department of Chemical and Materials Engineering, University of Nevada-Reno, Reno, Nevada 89557, USA

[b]Department of Materials Science, California Institute of Technology, Pasadena, CA 91125, USA

[c]I. Physikalisches Institut, University of Goettingen, 37077 Goettingen, Germany

[d]Materials and Process Simulation Center, California Institute of Technology, Pasadena, CA 91125, USA.

Emails: qia@unr.edu ; wlj@caltech.edu ; wag@caltech.edu

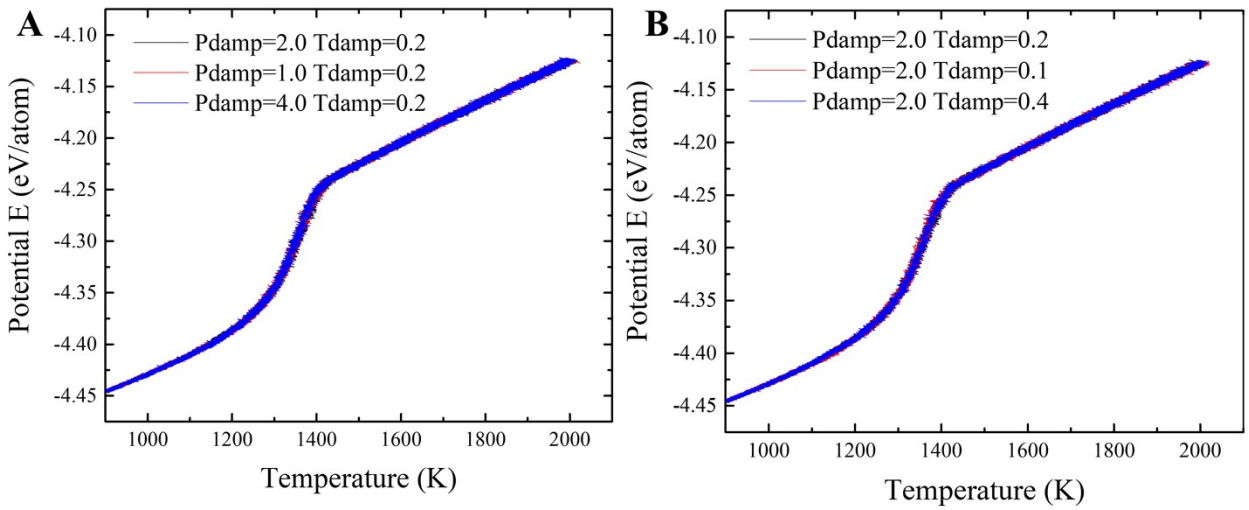

Fig. S1. The G-phase melting using different damping constants for barostat and thermostat. (A) Fixing thermostat damping constant to 0.2 ps and varying barostats damping constant from 1.0 to 4.0 ps. (B) Fixing barostats damping constant to 2.0 ps and varying thermostats damping constant from 0.1 to 0.4 ps.

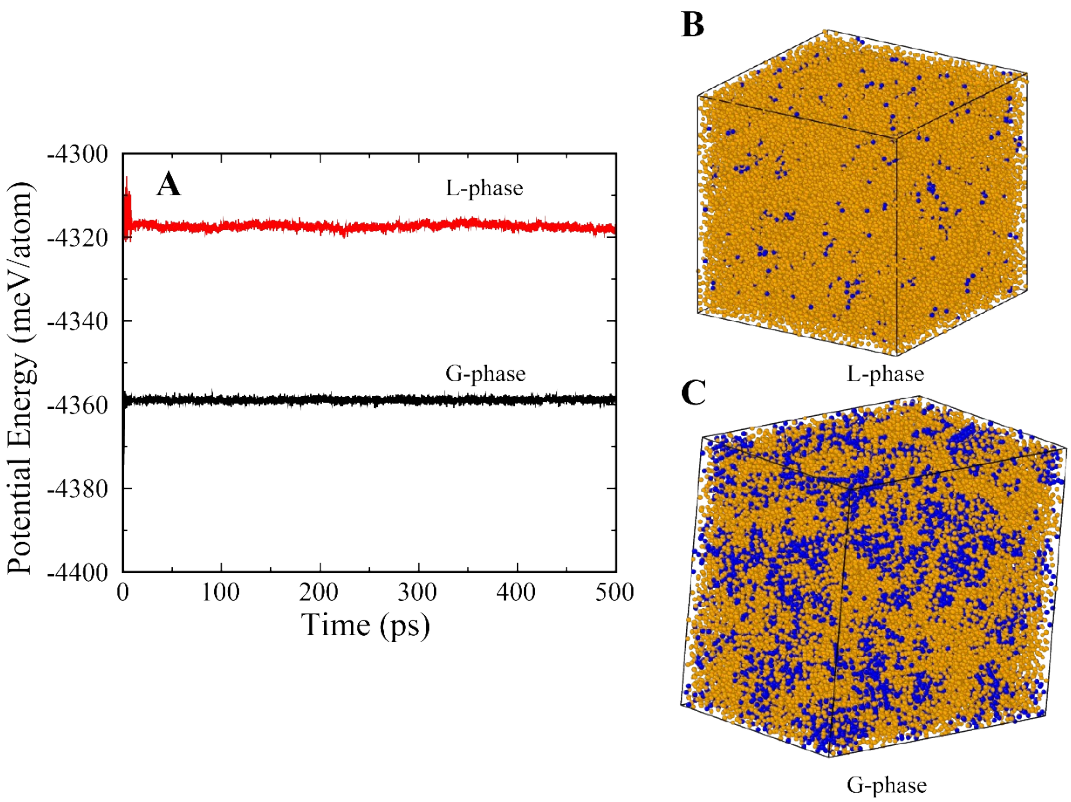

Fig. S2. The L-G transition of Cu_2Zr composition using the 2nd EAM potential.[1] The formed L-phase and G-phase from the 1st EAM potential were further equilibrated for another 500 ps using the 2nd potential. For comparison, the potential energy (PE) for Laves phase is -4382 meV/atom at 900 K. (A) The PE curves for both L-phase and G-phase. (B) The L-phase characterized using Honeycutt-Anderson analysis at 900 K. (C) The G-phase characterized using Honeycutt-Anderson analysis at 900 K. The icosahedral and liquid atoms are represented by purple and yellow balls, respectively.

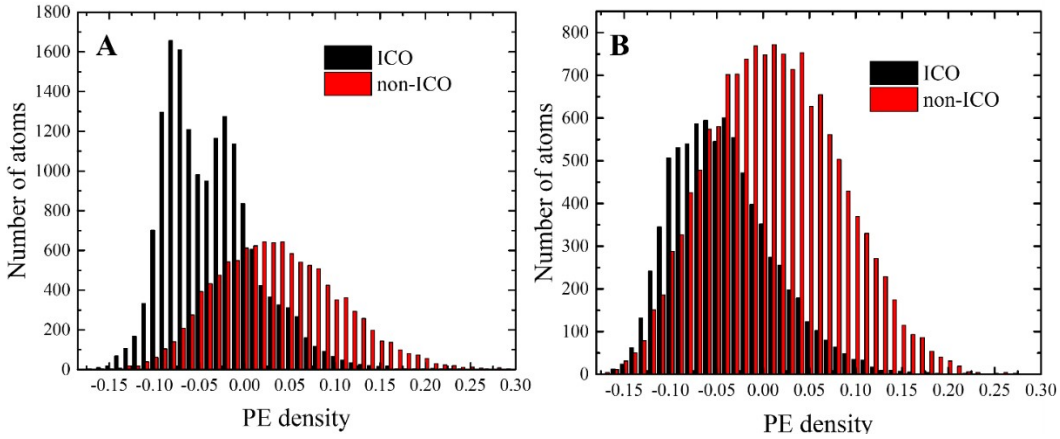

Fig. S3. The PE density distribution for (A) Cu_2Zr and (B) Cu_7Zr_3 G-phase structures at room temperature.

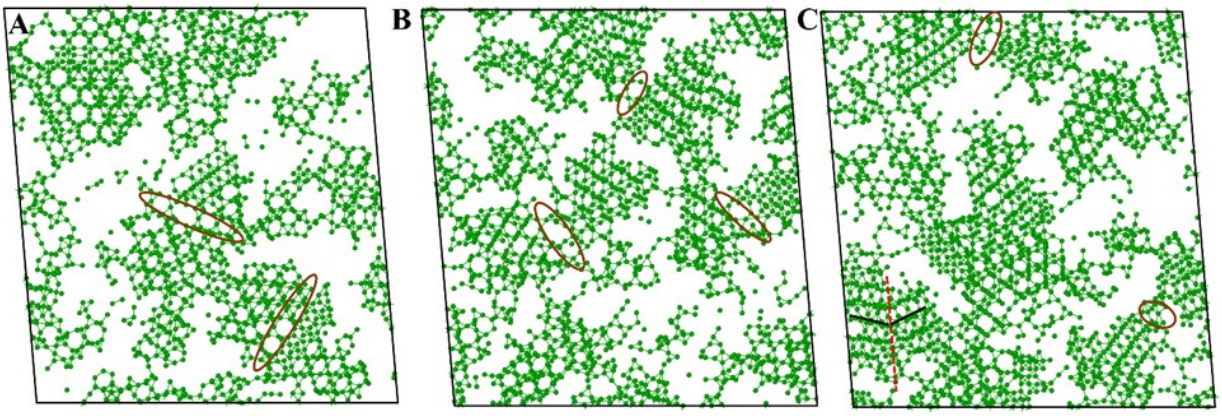

Fig. S4. The icosahedral atoms in Cu_2Zr at 300 K and they are displayed in three slabs (A, B, C) with a thickness of 8 Å in the same bulk structure. The first minimum of RDF (3.4 Å) is used to determine whether the icosahedral atoms are bonded or not. Only Cu atoms are displayed since Zr is not determined to be an icosahedral atom in Laves phase due to its higher coordination number (>12).

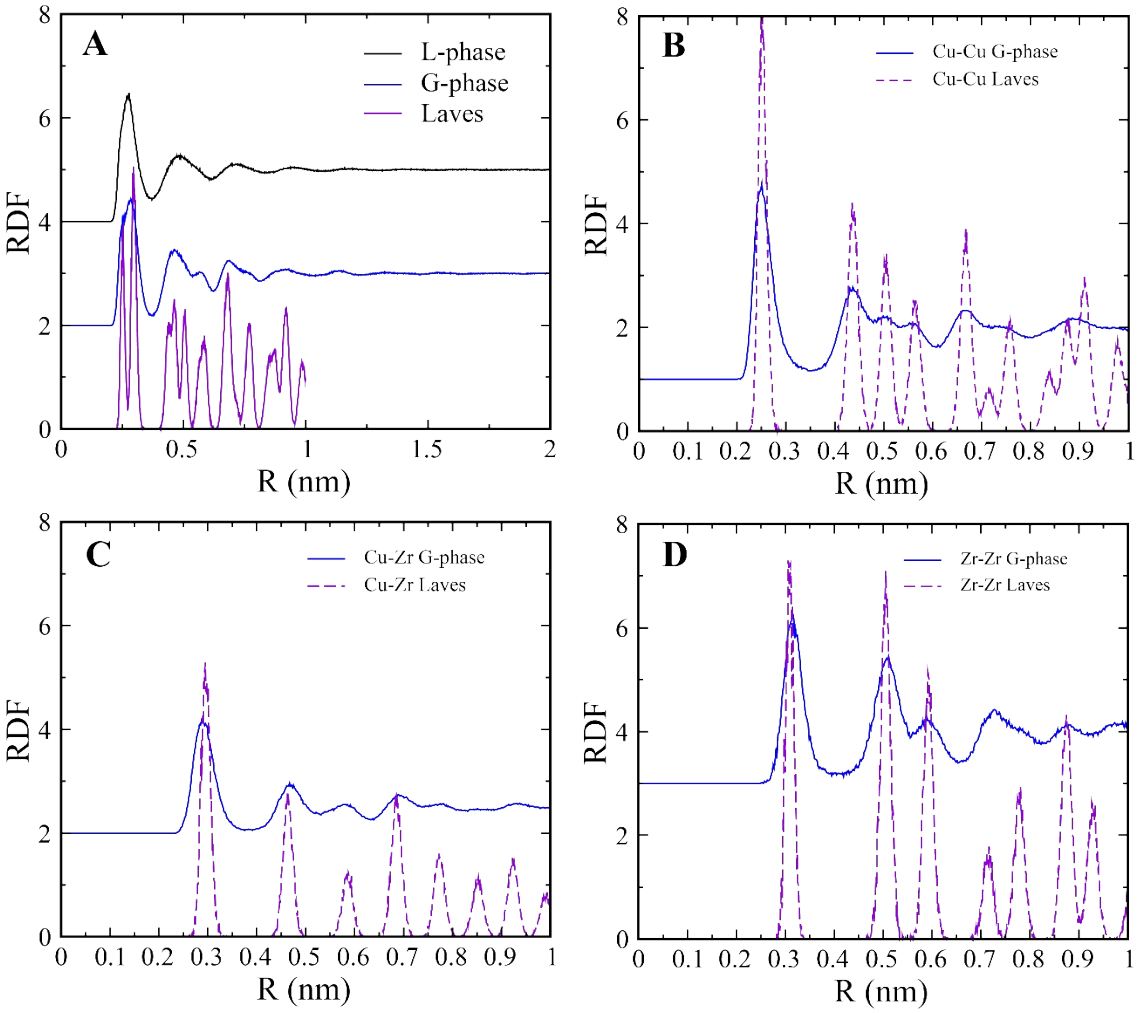

Fig. S5. RDF analysis of Cu_7Zr_3. (A) Total RDF of all three phases. (B-D) The comparison of partial RDF for G-phase and Laves phase: Cu-Cu (B), Cu-Zr (C), and Zr-Zr (D).

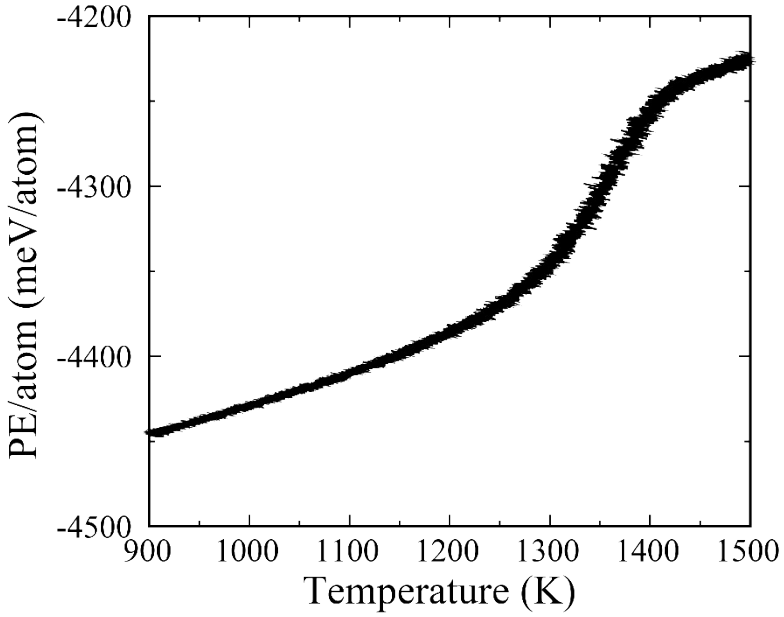

Fig. S6. Remelting of G-phase from 900 K to 1500 K. The melting occurs at ~1300 K.

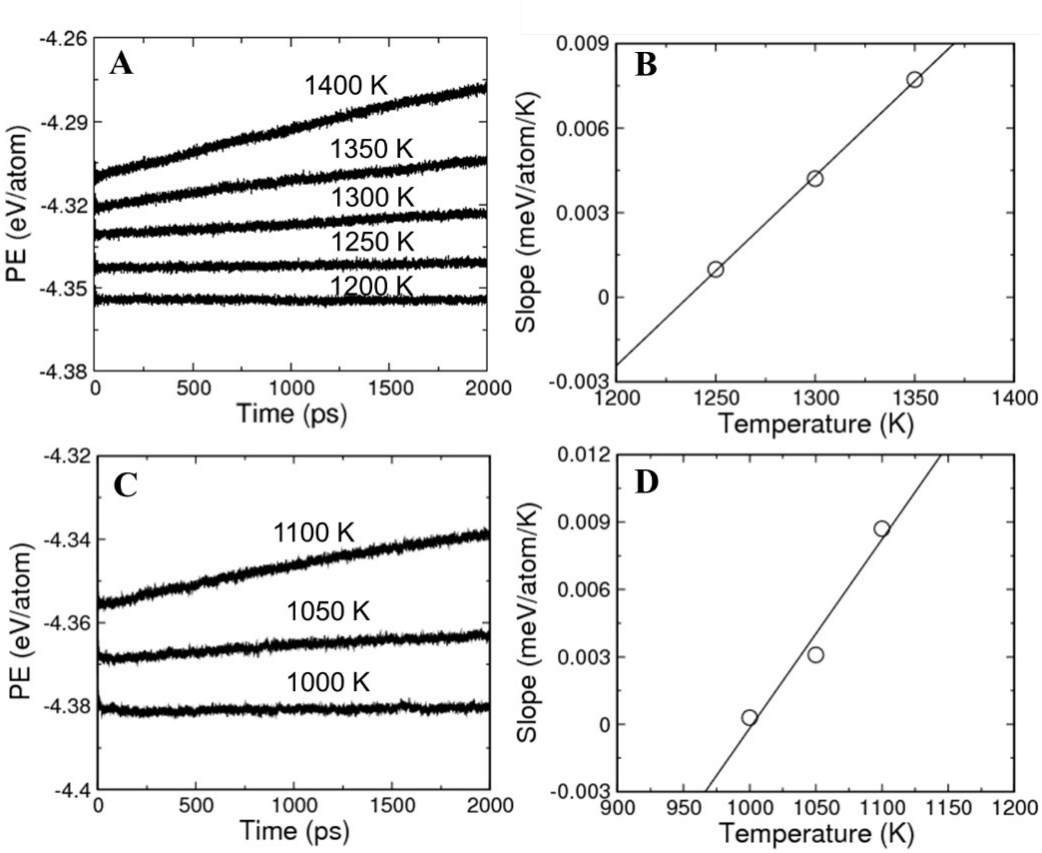

Fig. S7. The two-phase coexistence simulation for the composition Cu_2Zr to determine the $T_{X,M}$ and $T_{G,M}$. (A) The PE curves for liquid-Laves coexistence simulation. (B) The slope of PE near $T_{X,M}$ from (A). (C) The PE curves for L-G coexistence simulation. (D) The slope of PE near $T_{G,M}$ from (C).

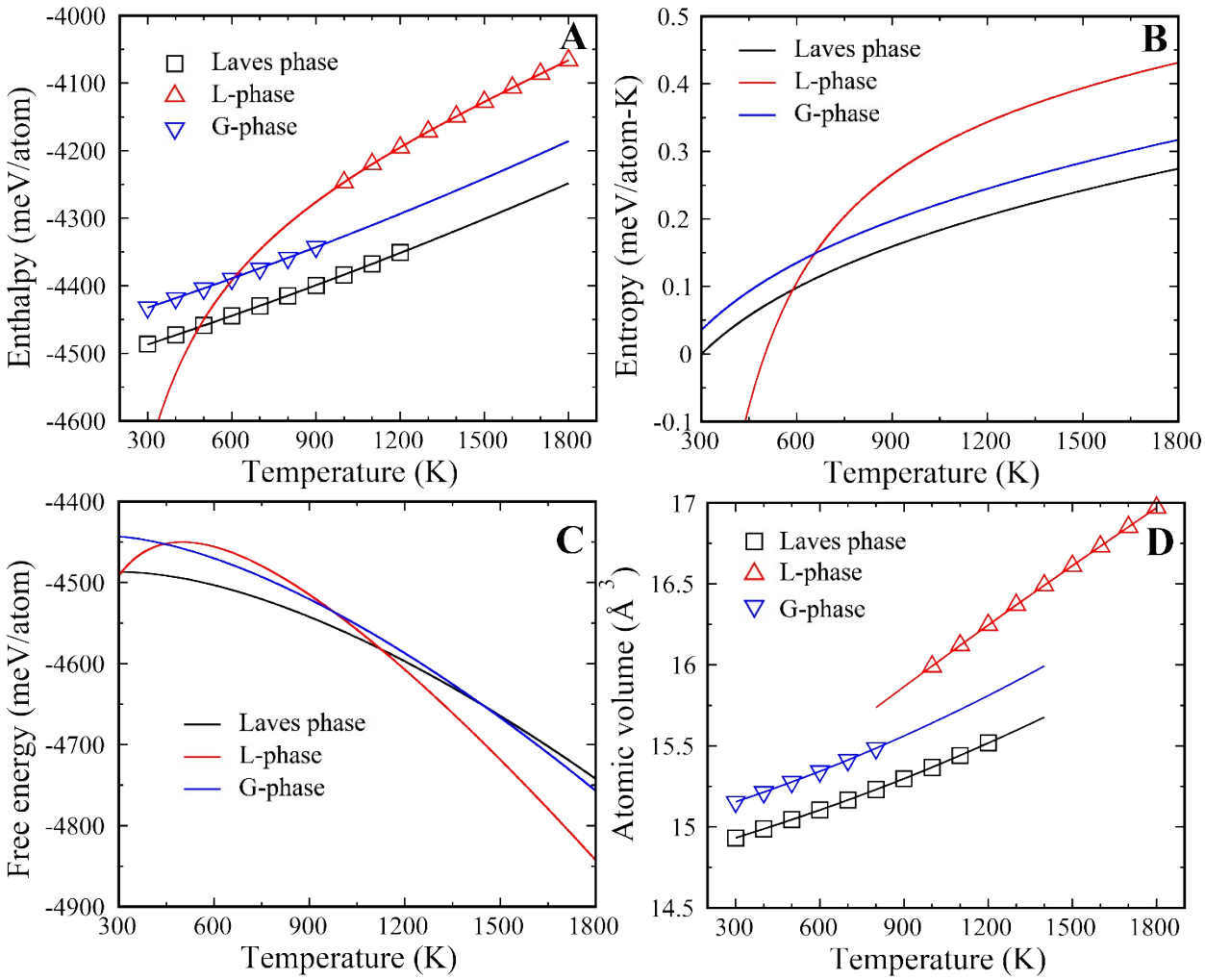

Fig. S8. Thermodynamic state functions for Cu_7Zr_3. (A) enthalpy, (B) entropy, (C) free energy, and (D) molar volume as a function of temperature.

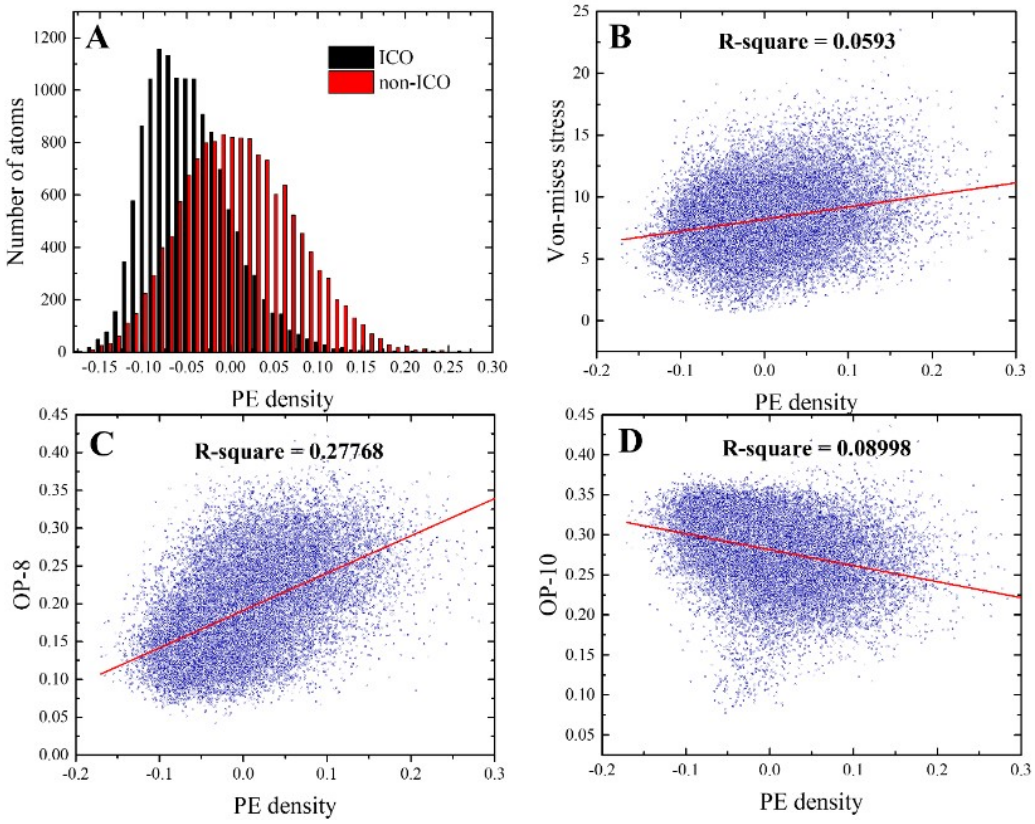

Fig. S9. The correlation analysis for Cu atoms in Cu_2Zr: (A) PE-density vs HA analysis, (B) PE-density vs Von-mises stress, (C) PE-density vs OP-8, and (D) PE-density vs OP-8.

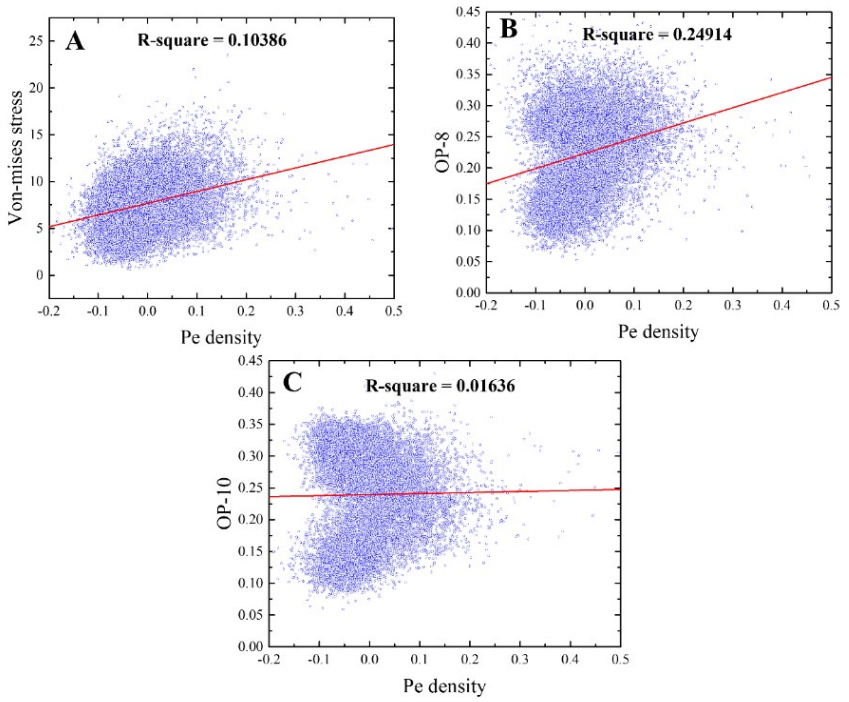

Fig. S10. The correlation analysis for Zr atoms in Cu_2Zr: (A) PE-density vs Von-mises stress, (B) PE-density vs OP-8, and (C) PE-density vs OP-8.

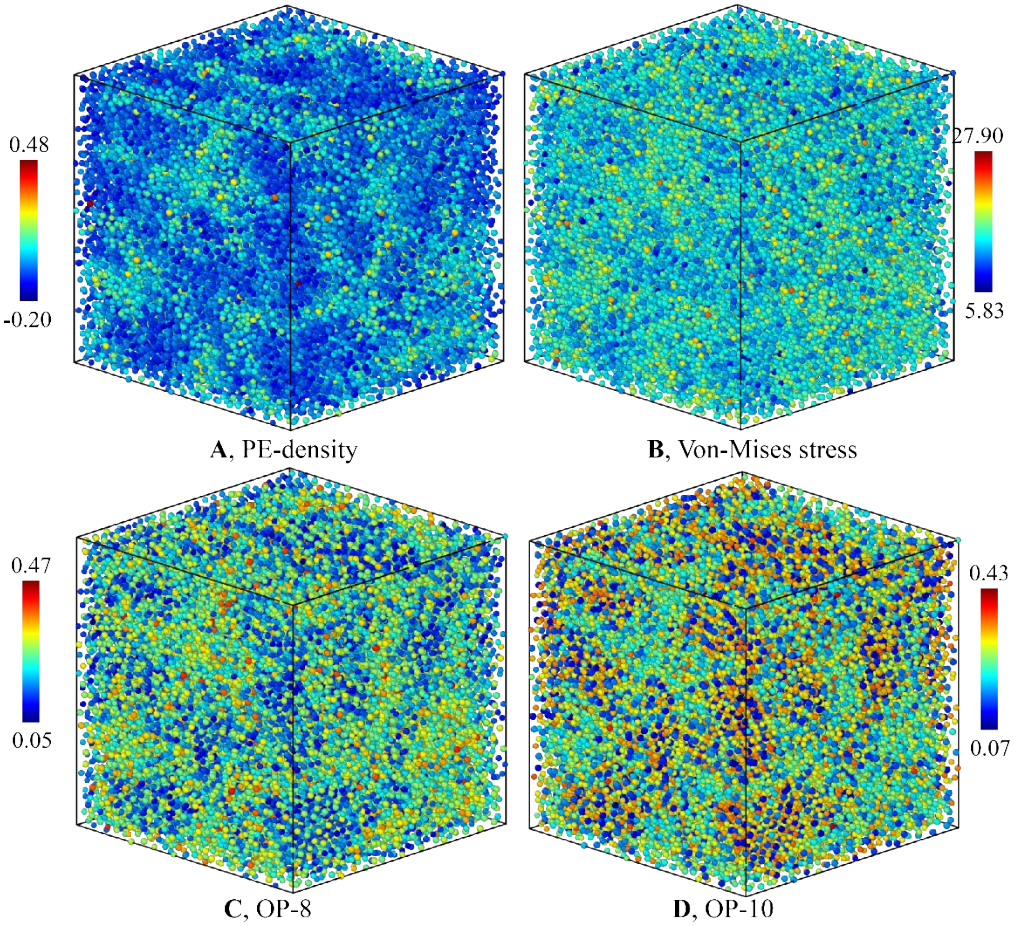

Fig. S11. Characterization of G-phase at 900 K for composition Cu_7Zr_3: (A) PE-density map, (B) Von-mises stress, (C) OP-8, and (D) OP-10.

References

[1] M. I. Mendelev, Y. Sun, F. Zhang, C. Z. Wang, and K. M. Ho, J. Chem. Phys., 2019, **151**, 214502.